# Narrow-Band Extreme-Ultraviolet Laser Radiation Tunable in the Range 90.5–95 nm

## Application to the Spectroscopy of $N_2$

W. Ubachs, K. S. E. Eikema, W. Hogervorst

Laser Centre, Department of Physics and Astronomy, Vrije Universiteit, De Boelelaan 1081, 1081 HV Amsterdam, The Netherlands
(Fax: +31-20/646-1459, e-mail: wimu@nat.vu.nl)

Abstract. Tunable, narrowband extreme ultraviolet radiation in the range 90.5–95 nm with only limited intensity variations is produced by frequency-tripling ultraviolet light from a frequency-doubled dye laser in a gas-jet of xenon. Acetylene gas is found to be an efficient medium for third-harmonic generation in this wavelength range as well. The extreme-ultraviolet radiation is applied in a spectroscopic study of the $b^1\Pi_u$, $v = 6$–8 and $v = 10$–12, $o^1\Pi_u$, $v = 0$ and $b'\,^1\Sigma_u^+$, $v = 9$ states of molecular nitrogen. From linewidth measurements a value $k_p = 6 \times 10^{10}$ s$^{-1}$ for the predissociation rate of the $b\,^1\Pi_u$, $v = 11$ state is deduced.

PACS: 42.65.Ky, 33.20.Ni, 95.30.Ky

In recent years various nonlinear optical wave-mixing techniques have been explored for the generation of coherent Extreme-UltraViolet (XUV) radiation at wavelengths below 100 nm. In particular, sum-frequency mixing processes in krypton and xenon gases were shown to be efficient because of strong resonance-enhancement effects at the atomic two-photon level [1]. Straightforward frequency tripling of the output of frequency-doubled dye lasers also gives access to the XUV, but is in principle less efficient. However, with the availability of powerful Nd:YAG lasers this is no longer a problem. Third-Harmonic Generation (THG) has some practical advantages. Firstly, only a single, frequency-doubled tunable laser is required. Secondly, an on-line calibration spectrum can always be recorded at the visible wavelength yielding a high absolute accuracy at the sextupled frequency in the XUV. Thirdly, continuous scans over larger wavelength ranges in the XUV are possible without changing dyes. In previous studies on THG in gaseous jets of xenon [2–5], the most efficient nonlinear medium for production of radiation in the range 90–100 nm, it was observed that large fluctuations in the conversion efficiency occur because of a resonance-enhancement effect of $ns$ and $nd$ autoionizing Rydberg states in the atom. In the present work it is demonstrated that also this disadvantage can be overcome.

By focusing intense UV-pulses at a position shifted from the jet centre in the forward direction a wide wavelength range is accessible with only limited variations in XUV yield.

The narrowband XUV radiation is applied for a study of selected excited vibronic states of $N_2$ in the range 90.5–95 nm. It is an extension towards shorter wavelengths of previous studies [6, 7] exploring the technique of 1 XUV + 1 UV two-photon ionization. The absorption spectrum of molecular nitrogen, the most abundant molecule in the earth atmosphere, has been subject of numerous investigations since the early work of Hopfield [8]. The congested and complicated spectrum in the XUV at wavelengths shorter than 100 nm was unraveled by the work of Lefebvre-Brion [9], Dressler [10] and Carroll and Collins [11]. An extensive analysis of perturbations in the vibronic structure of the valence and Rydberg states was performed by Stahel et al. [12], but rotational state dependences of the interactions and heterogeneous perturbations were not yet accounted for. Examples of rotational state-dependent perturbations for a limited number of vibronic states were published by Yoshino et al. [13, 14].

The ongoing research into the spectroscopy of $N_2$ is partly motivated by the need for accurate data to interprete extreme ultraviolet atmospheric light scattering processes, such as the terrestrial airglow. Also in the atmospheres of the planetary satellites Titan and Triton nitrogen is the major constituent and the analysis of Voyager-1 observations of XUV-emissions from these atmospheres is still in progress [15, 16]. Future space missions carrying higher resolution XUV-spectroscopic equipment are scheduled for flight in 1994 [17]. These applications require accurate data on absorption oscillator strengths [18], electron scattering cross-sections [19, 20], excited-state emissions [21], predissociation rates [6], collisional deactivation rates and line positions. The present study contributes to this field with accurate measurement and absolute wavelength calibration of line positions, particularly for the bandhead regions of bands that were less well resolved in previous studies [11, 13]. Spectroscopic analyses of excited states $b^1\Pi_u$, $v = 6$–8 and 10–12, $o^1\Pi_u$, $v = 0$ and $b'\,^1\Sigma_u^+$, $v = 9$ of $N_2$ are presented. From observed spectral linewidths lower limits to the excited-state lifetimes are deduced.

## 1 Production of XUV Radiation: Third-Harmonic Generation in Xe and $C_2H_2$

Narrowband XUV radiation is produced by frequency tripling light from a frequency-doubled dye laser pumped by an injection seeded Nd:YAG laser. The wavelength range 90.5–94.5 nm can be covered using fluorescein dye in a basic methanol solution; at longer wavelengths rodamine-6G dye is used. Frequency tripling takes place in a free expanding gas jet near the opening orifice (diameter 1 mm) of a home-built piezo-electric pulsed valve, based on a design of Proch and Trickl [22]. The conditions for THG are as follows: UV-light intensity 8 MW (40 mJ in 5 ns) focused with a $f = 20$ cm lens in a waist of 10–20 µm, resulting in a confocal parameter on the order of the interaction length of 1 mm. In our setup the intensity of the XUV-laser beam cannot be measured by direct counting of XUV photons, as it is overlapped by a UV-laser beam a million times stronger. Instead, the ionization current of a probe gas, for which propylene ($C_3H_6$) is chosen, is monitored. The XUV-induced photoionization of propylene was found to be independent of wavelength [23] in the range 105–120 nm and it is assumed here that it remains constant towards shorter wavelengths.

The efficiencies for THG are measured for xenon and acetylene as non-linear media. For xenon a pressure of 3 bar is used as backing pressure for the pulsed valve. Under these conditions optical breakdown in the medium is easily induced. This phenomenon results in intense light bursts emanating from the tripling zone; moreover pulses of broadband soft x-ray radiation are found to ionize the molecular beam. Lowering the pressure in the tripling zone, effected by decreasing the travel of the plunger in the pulsed valve, then prevents breakdown to occur. In the pressure regime just below breakdown conditions the most efficient generation of narrowband XUV radiation is observed. In studies, where XUV radiation is applied for spectroscopy, these optimum conditions are usually chosen. The wavelength dependence of the XUV intensity, covering the range of the dye fluores-

cein, is shown in Fig. 1 for Xe and $C_2H_2$. The conversion efficiency curves show that in the present setup the XUV wavelength can be continuously tuned in the relatively wide wavelength range of 90.5–94.3 nm, without changing the dye in the laser and with intensity variations of only 50%. The XUV intensity in Fig. 1 is recorded by averaging over 2 shots per frequency setting; a shot-to-shot noise for the XUV-laser source of 20% may be deduced. The wavelength of 90.5 nm is the shortest that can be generated by sextupling a dye laser pumped by the green output of the Nd:YAG laser. Shorter wavelengths are generated by pumping dyes with the UV output of the Nd:YAG laser, but at the cost of intensity.

The observed tripling curve for Xe markedly differs from that in some previous studies [4–5], where clear evidence was seen of resonance-enhanced THG by $ns$ and $nd$ autoionizing Rydberg states between the $^2P_{3/2}$ and $^2P_{1/3}$ ionization limits. The generated intensity $I_{3\omega}$ in THG is proportional to:

$$I_{3\omega} \propto N^2 |\chi^{(3)}(3\omega, \omega, \omega, \omega)|^2 F(b\Delta k) I_\omega^3, \tag{1}$$

with N the density of the medium and $I_\omega$ the intensity of the fundamental beam. $F(b\Delta k)$ is the so-called phase-matching integral [2, 3, 24], which strongly depends on the focusing geometry. The third-order nonlinear susceptibility $\chi^{(3)}$ may be approximated by a single dominant resonance term

$$\chi^{(3)}(3\omega, \omega, \omega, \omega)$$
$$= \sum_{1,2,3} \frac{\langle 0| \mu |1\rangle \langle 1| \mu |2\rangle \langle 2| \mu |3\rangle \langle 3| \mu |0\rangle}{(\omega - \omega_1)(2\omega - \omega_2)(3\omega - \omega_3 - i\Gamma)}, \tag{2}$$

where states $|i\rangle$, $i = 1, 2, 3$ ly at the $i$-photon level and $|0\rangle$ is the atomic ground state. $\Gamma$ represents the damping rate related to resonance levels in the medium; in the case of xenon only occurring at the three-photon level. There, $ns$ and $nd$ Rydberg states give rise to resonance enhancement. The generated frequency $\omega_{XUV} = 3\omega$ is reabsorbed in the
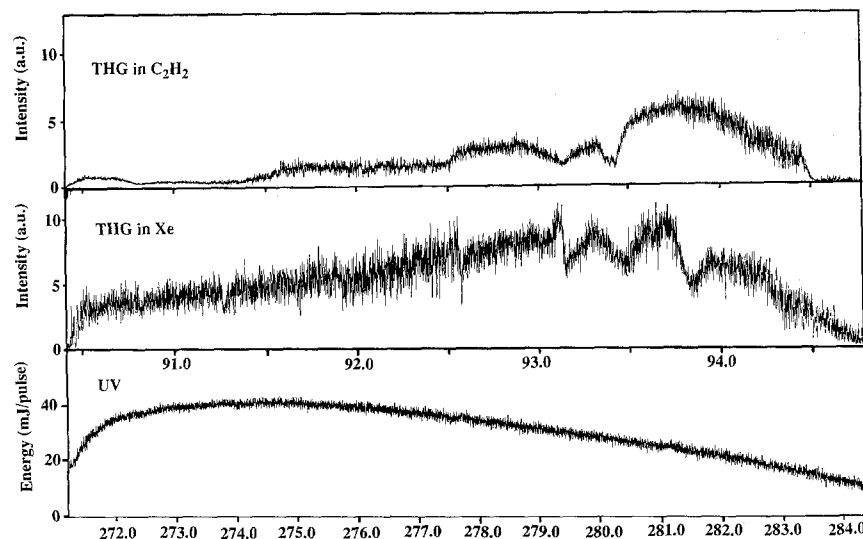


**Fig. 1.** Yield curves of extreme ultraviolet radiation generated by frequency tripling light in the wavelength range covered by a fluorescein dye laser after frequency doubling. *Upper curve:* $C_2H_2$ as tripling medium; *middle curve:* xenon as tripling medium. Intensity scales are in arbitrary units and are the same. *Lower curve:* UV-intensity in mJ/pulse

medium as the $ns$ and $nd$ states correspond to 1-photon XUV resonances. Moreover, the phase-matching function $F(b\Delta k)$ depends on resonances in the medium, because here the dispersion changes sign. A delicate interplay of these competing effects near the resonances determines the intensity of the generated third harmonic. At the outward edge of the gas-jet reabsorption is lower and optimum conditions for THG are obtained. In the present study an optimum conversion efficiency with only limited intensity variations is found when the focus is displaced 1 mm in the forward direction from the centre of the jet (the orifice diameter is also 1 mm). Also a washing out of the typical resonance structure is observed.

In addition to xenon other gaseous media have been tried. It is found that many gases ($CH_4$, $O_2$, $N_2$, CO, $CO_2$, $C_2H_2$, $NH_3$, $H_2S$) have an appreciable non-linear susceptibility and may be used for THG, generally less efficient than xenon, and in some cases large wavelength dependent variations in the production effiency may occur [4, 25]. Acetylene is efficient, allows for a wide tunability, and is reinvestigated in the present work (see Fig. 1). The conditions at which $C_2H_2$ is used differ from those used for xenon. The backing pressure in the valve is at maximum 1.5 bar, because acetylene liquifies at higher pressures. Even at the highest pressures that can be reached in the interaction zone optical breakdown does not occur. Under these conditions, where XUV production is at maximum, white fluorescence light is observed from the tripling region. Particularly in the range $\lambda > 93.5$ nm the cheaper acetylene gas may be used for efficient production of XUV by THG.

## 2 Application of Narrowband XUV Radiation: Spectroscopy of $N_2$

### 2.1 Experimental

The experimental setup is the same as that of the previous study on the $c_4' \, {}^1\Sigma_u^+ \, v = 0$ Rydberg state of $N_2$ [7]. A skimmed and well-defined pulsed molecular beam of pure nitrogen is perpendicularly intersected by temporally and spatially overlapping XUV and UV laser light. Nitrogen molecules are resonantly excited by the XUV photons and subsequently ionized by the intense UV light. Thus XUV-excitation spectra are recorded by $1 + 1$ two-photon ionization. $N_2^+$ ions are detected using a time-of-flight mass selector. The sensitivity of this method allows for spectroscopic studies to be performed in a crossed-beam configuration with local pressures of $10^{-4}$–$10^{-5}$ Torr in the interaction zone. This region is 30 cm away from the focus point where the XUV light is generated. As a consequence, the molecules are excited under conditions of diverging light beams with a diameter of about 1 cm at the interaction zone. Under these conditions Doppler-broadening effects are limited to 0.02 cm$^{-1}$.

The frequency in the XUV range is calibrated by a computerized interpolation of an $I_2$-absorption spectrum [26], that is simultaneously recorded with the visible output of the dye laser. A relative accuracy of 0.05 cm$^{-1}$ and an absolute accuracy of 0.1 cm$^{-1}$ for the observed line positions in the XUV is estimated.
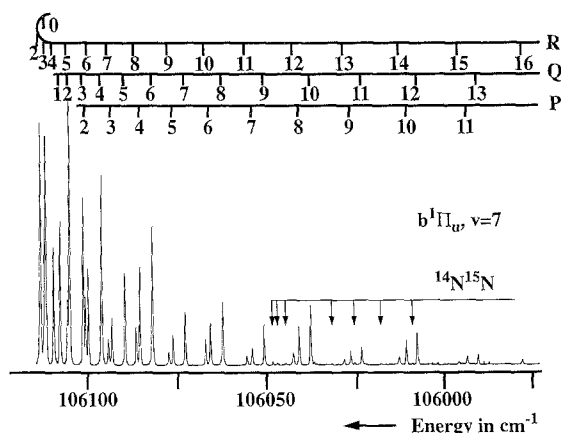


**Fig. 2.** Spectrum of the $b\,{}^1\Pi_u$–$X\,{}^1\Sigma_g^+(7,0)$ band of $N_2$. Lines of the ${}^{14}N^{15}N$ isotopomer are indicated separately
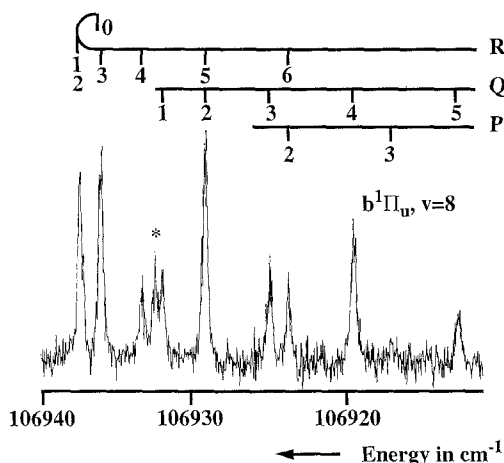


**Fig. 3.** Spectrum of the $b\,{}^1\Pi_u$–$X\,{}^1\Sigma_g^+(8,0)$ band of $N_2$

### 2.2 Results

XUV-excitation spectra have been recorded in the range 90.5–95 nm, covered mainly by the sextupled output of the dye laser running on fluorescein dye. Moreover, in order to complete a study on the $b\,{}^1\Pi_u$, $v$ vibronic states the $v = 6$ level was excited using rhodamine 6G as dye. In transitions to the $b\,{}^1\Pi_u$ state the bandhead parts are better resolved than in previously published work [11, 13]. Examples of transitions to $v = 7, 8, 11$ and 12 are shown in Figs. 2–5. Because transition frequencies have been tabulated before in Table 1 only experimental values of derived rotational constants are presented. The excited state energies are equated to:

$$E_{\Pi^+} = \nu_0 + BJ(J+1) - DJ^2(J+1)^2 + qJ(J+1), \quad (3)$$

$$E_{\Pi^-} = \nu_0 + BJ(J+1) - DJ^2(J+1)^2, \quad (4)$$

where $\nu_0$ is the band origin, $B$ the rotational constant, $D$ the centrifugal distortion constant and $q$ the $\Lambda$-doubling parameter. The rotational energy levels of the $X\,{}^1\Sigma_g^+$, $v = 0$ electronic ground state are calculated from the accurate molecular constants of Bendtsen [27]. For the $b\,{}^1\Pi_u$, $v = 8$, 10 and 11 states only the lowest rotational states have been excited, but still accurate values for the band origins can be determined.

**Table 1.** Spectroscopic constants for the states of $N_2$. All values in $cm^{-1}$. Parameters denoted with $(a)$ are fixed in the minimization routine

| | | $\nu_0$ | $B$ | $D$ | $q$ | Highest $J$ |
|---|---|---|---|---|---|---|
| $b'\,^1\Sigma_u^+,$ | $v = 9$ | $110196.91 \pm 0.03$ | $1.1244 \pm 0.0004$ | $1.52 \pm 0.09 \times 10^{-5}$ | | $R(21), P(22)$ |
| $b\,^1\Pi_u,$ | $v = 6$ | $105346.02 \pm 0.01$ | $1.3624 \pm 0.0002$ | $1.47 \pm 0.08 \times 10^{-5}$ | $1.7 \pm 0.1 \times 10^{-3}$ | $R(17), Q(16), P(13)$ |
| | $v = 7$ | $106109.63 \pm 0.03$ | $1.3412 \pm 0.0005$ | $1.0 \times 10^{-5\,(a)}$ | | $R(10), Q(10), P(10)$ |
| | $v = 8$ | $106933.06 \pm 0.03$ | $1.324 \pm 0.001$ | $1.0 \times 10^{-5\,(a)}$ | | $R(4), Q(8), P(3)$ |
| | $v = 10$ | $108371.69 \pm 0.04$ | $1.213 \pm 0.002$ | $1.0 \times 10^{-5\,(a)}$ | | $R(7), Q(5), P(4)$ |
| | $v = 11$ | $109119.71 \pm 0.04$ | $1.193 \pm 0.002$ | $1.0 \times 10^{-5\,(a)}$ | | $R(7), Q(5), P(4)$ |
| | $v = 12$ | $109831.27 \pm 0.03$ | $1.1479 \pm 0.0008$ | $-7 \pm 3 \times 10^{-6}$ | | $R(14), Q(16), P(12)$ |
| $o\,^1\Pi_u,$ | $v = 0$ | $105682.96 \pm 0.03$ | $1.6930 \pm 0.0008$ | $1.3 \pm 0.3 \times 10^{-5}$ | $-5.6 \pm 0.3 \times 10^{-3}$ | $R(12), Q(16), P(15)$ |

**Table 2.** Observed line positions (in $cm^{-1}$) of the $b\,^1\Pi_u - X\,^1\Sigma_g^+(7,0)$ band of the $^{14}N^{15}N$ isotope

| Transition frequency | Assignment |
|---|---|
| 106048.79 | $R(0), R(3)$ |
| 106047.51 | $R(1), R(2)$ |
| 106045.17 | $R(4)$ |
| 106032.26 | $Q(4)$ |
| 106026.08 | $Q(5)$ |
| 106018.49 | $Q(6)$ |
| 106009.90 | $Q(7)$ |

Derived molecular constants: $\nu_0 = 106044.75 \pm 0.08\ cm^{-1}$, $B = 1.300 \pm 0.002\ cm^{-1}$; $D$ is fixed at $1.0 \times 10^{-5}\ cm^{-1}$
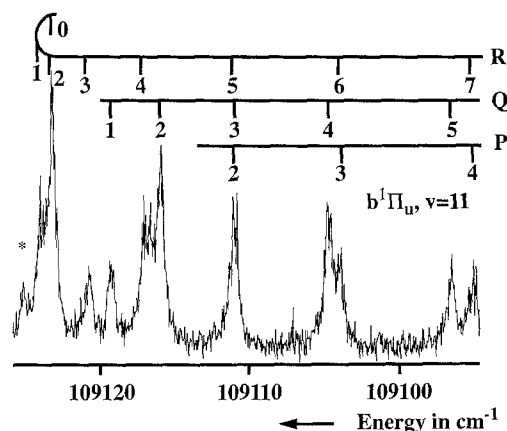


**Fig. 4.** Spectrum of the $b\,^1\Pi_u - X\,^1\Sigma_g^+(11,0)$ band of $N_2$
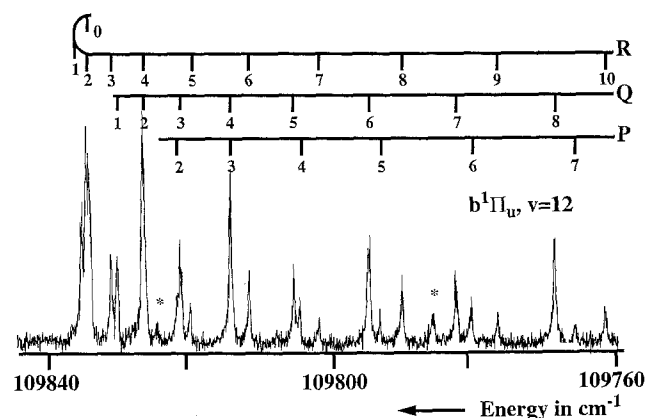


**Fig. 5.** Spectrum of the $b\,^1\Pi_u - X\,^1\Sigma_g^+(12,0)$ band of $N_2$. Lines marked with $(*)$ are identified as the $P(19)$ and $P(20)$ transitions of the $b'\,^1\Sigma_u^+ - X\,^1\Sigma_g^+(9,0)$ band

The $b\,^1\Pi_u$, $v = 6$ state is found not to be affected by a homogeneous perturbation, at least up to $J = 18$. In the $b\,^1\Pi_u$, $v = 6$ and $o\,^1\Pi_u$, $v = 0$ states a $\Lambda$-doubling is found that gives rise to splitting in $\Pi^+$-levels (observed in $R$ and $P$ branches) and $\Pi^-$-levels (observed in the $Q$-branch). In $b\,^1\Pi_u$, $v = 6$ the $\Pi^+(J)$ levels are shifted upward, with respect to the $\Pi^-(J)$ levels, whereas in the $o\,^1\Pi_u$, $v = 0$ state the opposite is the case.

For higher rotational states of $b\,^1\Pi_u$, $v = 7$ ($J > 10$) a marked upward shift with respect to calculated values (based on the constants of Table 1) is found. This is caused by a homogeneous perturbation by the $o\,^1\Pi_u$, $v = 0$ state. Rotational states up to $J = 10$ are still well represented by the parameters in the minimization routine. In the line positions of the $o\,^1\Pi_u - X\,^1\Sigma_g^+(0,0)$ band a corresponding downward shift is found for $J > 16$. These higher $J$-values have been left out of the fit. The excitation spectrum of the $b\,^1\Pi_u$, $v = 7$ state is so strong that several lines of the $^{14}N^{15}N$ isotope are also observed in natural abundance (see Fig. 2). The line positions and derived molecular constants are listed in Table 2.

In the $b\,^1\Pi_u$, $v = 12$ state the energies up to $J = 16$ are accurately represented by the parameters listed in Table 1, although the negative value for the centrifugal distortion parameter is unphysical. The upward shift of the higher $J$-states represented by this negative sign may be interpreted in terms of a homogeneous interaction with the $o\,^1\Pi_u$, $v = 2$ state with a crossing at $J = 22$ [13].

Although most of the $b\,^1\Pi_u$ states are known to be perturbed, either by homogeneous or by heterogeneous interactions, nevertheless, all transition frequencies up to the highest $J$-values covered by the present analysis can be calculated within $0.1\ cm^{-1}$ on the basis of the parameters given in Table 1. These constants may be reliably used for the modelling of spectra of $N_2$ at low temperatures, as often found in outer-space conditions.

At the short wavelength side of the XUV range accesible in the present setup, at $\lambda = 90.7$ nm, the $b'\,^1\Sigma_u^+ - X\,^1\Sigma_g^+(9,0)$ band is strongly excited. For the $b'\,^1\Sigma_u^+$, $v = 9$ state no values for line positions, which are listed in Table 3, have been reported before. This particular state is important for the interpretation of XUV-emission features in molecular nitrogen. In rotationally unresolved fluorescence studies, after excitation by synchrotron radiation, this state was found to be the strongest emitter in the range 90–95 nm [28] and the third strongest emitting state, after the $b\,^1\Pi_u$, $v = 1$ and $c_4'\,^1\Sigma_u^+$, $v = 0$, in the entire XUV region. The data are again fitted to expression (4), that also holds for a $^1\Sigma^+$ state and
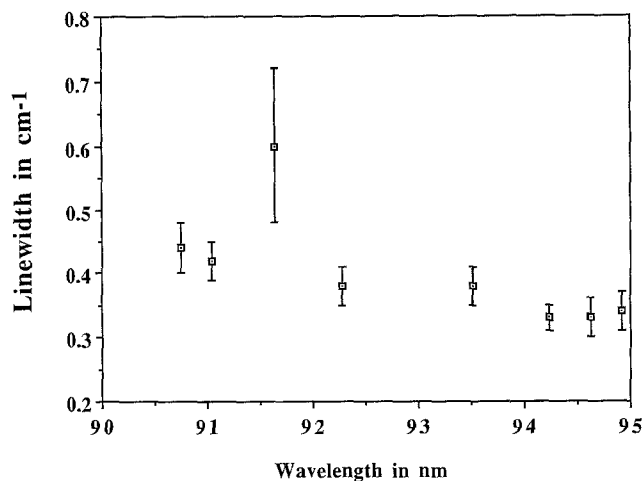
**Table 3.** Observed line positions (in $cm^{-1}$) of the $b'\,^1\Sigma_u^+\!-\!X\,^1\Sigma_g^+(9,0)$ band and deviations from a fit to expression(4)

| $J$ | $R(J)$ | | $P(J)$ | |
|---|---|---|---|---|
| | Observed | Obs.-calc. | Observed | Obs.-calc. |
| 0 | 110198.94 | −0.22 | | |
| 1 | 110199.47 | −0.21 | 110192.78 | −0.15 |
| 2 | 110198.39 | −0.07 | 110187.19 | −0.03 |
| 3 | 110195.43 | −0.09 | 110179.65 | −0.13 |
| 4 | 110190.78 | −0.06 | 110170.67 | 0.06 |
| 5 | 110184.45 | 0.03 | 110159.65 | −0.06 |
| 6 | 110176.35 | 0.08 | 110147.08 | 0.01 |
| 7 | 110166.40 | 0.02 | 110132.69 | −0.01 |
| 8 | 110154.91 | 0.15 | 110116.68 | 0.08 |
| 9 | 110141.55 | 0.16 | 110098.77 | 0.00 |
| 10 | 110126.28 | 0.01 | 110079.33 | 0.14 |
| 11 | 110109.55 | 0.14 | 110058.00 | 0.12 |
| 12 | 110090.97 | 0.17 | 110034.82 | 0.00 |
| 13 | 110070.39 | −0.05 | 110010.11 | 0.09 |
| 14 | 110048.27 | −0.01 | 109983.49 | 0.01 |
| 15 | 110024.43 | −0.01 | 109955.17 | −0.01 |
| 16 | 109998.60 | −0.20 | 109925.12 | −0.01 |
| 17 | 109971.40 | 0.01 | 109893.19 | −0.14 |
| 18 | 109942.12 | −0.09 | 109859.65 | −0.12 |
| 19 | 109911.27 | 0.02 | 109824.30 | −0.15 |
| 20 | 109878.69 | 0.18 | 109787.27 | −0.09 |
| 21 | 109844.30 | 0.31 | 109748.33 | −0.17 |
| 22 | | | 109708.12 | 0.25 |



**Fig. 6.** Linewidths, as observed for isolated rotational lines in selected bands $[b'\,^1\Sigma_u^+\!-\!X\,^1\Sigma_g^+(9,0)$, $o\,^1\Pi_u\!-\!X\,^1\Sigma_g^+(0,0)$ and $b\,^1\Pi_u\!-\!X\,^1\Sigma_g^+(v',0)$ for $v' = 6$–12] of $N_2$, as a function of the wavelength of the bandhead

the resulting molecular constants are included in Table 1. It appears that the rotational structure of the $b'\,^1\Sigma_u^+$, $v = 9$ state is unperturbed up to the highest $J$-value observed: $J = 22$. As such it is one of the few unperturbed excited states of $N_2$.

### 2.3. XUV Bandwidth and Observed Linewidths

In a previous study, the bandwidth of the XUV-laser source was carefully examined [29] and a value of $0.32 \pm 0.04$ $cm^{-1}$ was specified. From the present spectra of molecular nitrogen linewidths are derived by fitting Voigt profiles to selected, well-resolved rotational lines. Average values for the widths in the bands vary from 0.33 $cm^{-1}$ to 0.44 $cm^{-1}$ with a typical uncertainty of 10%. These spectral linewidths are presented in Fig. 6 as a function of wavelength. If the one point at 91.7 nm is neglected (see below) we find a slope with a decrease of 30% over the range 90.7 nm to 95 nm. This variation in XUV bandwidth is connected to the bandwidth of the laser in the visible. The bandwidth of the Quanta-Ray PDL-3 dye laser depends on wavelength. A difference of 35% between 540 nm and 590 nm is specified, with narrower bandwidths at longer wavelengths [30]. As in the non-linear processes of frequency doubling and third-harmonic generation, the bandwidth of the fundamental procreates into the harmonis an increasing bandwidth of the XUV source from 0.30 $cm^{-1}$ at $\lambda = 96$ nm to 0.44 $cm^{-1}$ at $\lambda = 90.5$ nm can be estimated. This is consistent with the observed slope in Fig. 6 and with the measurement of spectral widths of rotational lines in the $L\,^1\Pi\!-\!X\,^1\Sigma^+(0,0)$ band of CO at 96.5 nm, where 0.30 $cm^{-1}$ is found [29]. At the highest pumping rates of the dye laser, in the domain where

40 mJ of UV is produced after frequency doubling, additional instrumental broadening effects are observed, related to gain saturation in the dye laser. Also, when the injection seeder of the Nd:YAG laser is turned off, strong broadening of the XUV radiation is observed.

### 2.4 Predissociation Rate of the $b\,^1\Pi_u$, $v = 11$ State

The observed linewidths, apart from the $b\,^1\Pi_u$, $v = 11$ state, further denoted as $b(11)$, reflect the estimated instrumental width. So it can be concluded that lifetime broadening is not observable; i.e. an upper limit for a broadening effect of 0.03 $cm^{-1}$ is obtained. This implies that the lifetimes $\tau$ of the excited states under investigation, except for $b(11)$, are all longer than 150 ps. For the $b'\,^1\Sigma_u^+$, $v = 9$ state a value of $\tau = 710$ ps has been reported [28], consistent with the present limit.

Although the error margin on the width of $b(11)$ is rather large, nevertheless, there is a strong indication for a line broadening effect related to predissociation of this state. Despite the low signal-to-noise ratio, the observed resonances show Lorentzian-like line shapes (see Fig. 4). From a deconvolution of the instrumental width [29] we obtain a value for the lifetime of the $b(11)$ state of 16 ps. As $b(11)$ has a dissociation yield of nearly 100% [20] this reflects a predissociation rate of $k_p = 6 \times 10^{10}$ $s^{-1}$.

The hypothesis of a high predissociation rate for $b(11)$ is supported by the weak intensity of the transition. It is known [6] that for $1 + 1$ two-photon ionization processes, as in emission processes, the signal intensity is proportional to the excited state lifetime. The oscillator strengths for transitions to the $b\,^1\Pi_u$, $v$ vibronic states were determined by James et al. [20]: 0.0003 for $v = 8$, 0.0032 for $v = 11$ and 0.0007 for $v = 12$. On the basis of these numbers a transition to $b(11)$ is expected a factor of 5 and 10 stronger than transitions to the $b\,^1\Pi_u$, $v = 12$ and $v = 8$, respectively. From a comparison of observed intensities in the spectra (see Figs. 3–5) it follows that this is not the case. The intensity of $b(11)$ equals that of $b\,^1\Pi_u$, $v = 8$, while the transition to $b\,^1\Pi_u$, $v = 12$ is

even stronger. These observations support the hypothesis of a fast predissociation rate for $b(11)$. This finding is not in contradiction with the result of James et al. [20], who found that for all $b\,^1\Pi_u$, $v > 7$ states predissociation *yields* are close to 100%. Even then predissociation *rates* may very well differ by orders of magnitude.

## 3 Conclusion and Outlook

In the present work a widely tunable, narrowband XUV-laser source with only limited intensity variations has been applied to spectroscopic studies of the nitrogen molecule. The earlier drawback of large wavelength-dependent intensity fluctuations of XUV, generated by third-harmonic processes in pulsed gas jets, has been circumvented by an optimized choice of focusing conditions. Lago et al. [2, 3] already mentioned the important influence of the location of the focus in the gas jet.

The highly sensitive method of 1 XUV+ 1 UV photoionization is ideally suited for high-resolution spectroscopy and for a determination of predissociation rates. However, it cannot provide reliable data on absorption cross-sections. For this purpose an on-line XUV/UV separation monochromator will be installed. Furthermore, work is in progress to replace the grating-based pulsed dye laser by an optical amplification system, seeded with narrowband cw-laser radiation. The resolution of the XUV spectrometer then will increase at least an order of magnitude.

## References

1. G. Hilber, A. Lago, R. Wallenstein: J. Opt. Soc. Am. B **4**, 1753 (1987)
2. A. Lago, G. Hilber, R. Wallenstein: Phys. Rev. A **36**, 3827 (1987)
3. A. Lago: Dissertation, University of Bielefeld (1987)
4. L.M. Tashiro: Ph.D. Thesis, Stanford University (1989)
5. R.H. Page, R.J. Larkin, A.H. Kung, Y.R. Shen, Y.T. Lee: Rev. Sci. Instrum. **58**, 1616 (1987)
6. W. Ubachs, L. Tashiro, R.N. Zare: Chem. Phys. **130**, 1 (1989)
7. P.F. Levelt, W. Ubachs: Chem. Phys. **163**, 263 (1992)
8. J.J. Hopfield: Phys. Rev. **36**, 789 (1930)
9. H. Lefebvre-Brion: Can. J. Phys. **47**, 541 (1969)
10. K. Dressler: Can. J. Phys. **47**, 547 (1969)
11. P.K. Carroll, C.P. Collins: Can. J. Phys. **47**, 563 (1969)
12. D. Stahel, M. Leoni, K. Dressler: J. Chem. Phys. **79**, 2541 (1983)
13. K. Yoshino, Y. Tanaka, P.K. Carroll, P. Mitchell: J. Mol. Spectrosc. **54**, 87 (1975)
14. K. Yoshino, D.E. Freeman: Can. J. Phys. **62**, 1478 (1984)
15. D.F. Strobl, D.E. Shemansky: J. Geophys. Res. **87**, 1361 (1982)
16. A.L. Broadfoot, S.K. Atreya, J.L. Bertaux et al.: Science **246**, 1459 (1989)
17. B.R. Sandel, A.L. Broadfoot: Bull. Am. Astron. Soc. **24**, 1035 (1989)
18. G. Stark, P.L. Smith, K. Yoshino, M.H. Stevens, K. Ito: J. Chem. Phys. **97**, 4809 (1992)
19. J.M. Ajello, G.K. James, B.O. Franklin, D.E. Shemansky: Phys. Rev. A **40**, 3524 (1989)
20. G.K. James, J.M. Ajello, B.O. Franklin, D.E. Shemansky: J. Phys. B **23**, 2055 (1990)
21. J.-Y. Roncin, F. Launay, K. Yoshino: J. Mol. Spectrosc. **134**, 390 (1989)
22. D. Proch, T. Trickl: Rev. Sci. Instrum. **60**, 715 (1989)
23. J.A.R. Samson, F.F. Marmo, K. Watanabe: J. Chem. Phys. **36**, 783 (1962)
24. G. Bjorklund: IEEE J. QE-**11**, 287 (1975)
25. W. Ubachs, L. Tashiro, R.N. Zare: Unpublished results
26. S. Gerstenkorn, P. Luc: *Atlas du spectre d'absorption de la molecule de l'iode entre* 148000–20000 cm$^{-1}$ (Editions du CNRS, Paris 1978)
27. J. Bendtsen: J. Raman Spectrosc. **2**, 133 (1974)
28. H. Oertel, M. Kratzat, J. Imschweiler, T. Noll: Chem. Phys. Lett. **82**, 552 (1981)
29. P.F. Levelt, W. Ubachs, W. Hogervorst: J. Chem. Phys. **79**, 7160 (1992)
30. Spectra Physics, data sheet on QuantaRay PDL-3 laser